Optik

International Journal for Light and Electron Optics

http://www.springer.com/materials/journal/12034

ISSN	Impact Factor	5-Year Impact Factor
0030-4026	0.742	0.690

Optik 140 (2017) 709–717

Contents lists available at ScienceDirect

Optik

journal homepage: www.elsevier.de/ijleo

Original research article

The effect of Al and In concentrations on the properties of electrodeposited Cu(In,Al)Se_2 using two electrode system without the addition of complexing agents

O. Meglali [a,b,*], A. Bouraiou [b], N. Attaf [c], M.S. Aida [c]

[a] Faculty of Sciences, Mohammed Boudiaf University, M'Sila 28000, Algeria
[b] Materials Science and Informatics Laboratory, Ziane Achour University, Djelfa 17000, Algeria
[c] Thin Films and Interfaces Laboratory, Department of Physics, Mentouri University, Constantine 25000, Algeria

ARTICLE INFO

Article history:
Received 27 January 2017
Received in revised form 19 April 2017
Accepted 20 April 2017

Keywords:
Thin films
Electrodeposition
Cu(In,Al)Se_2
x ratio

ABSTRACT

Chalcopyrite Cu(In,Al)Se_2 thin films were deposited by electrodeposition process onto ITO coated glass substrates from de-ionized water solution consisting of $CuCl_2$, $InCl_3$, $AlCl_3$ and SeO_2 precursors. The effect of Al and In concentrations in precursor solutions on the properties of Cu(In,Al)Se_2 films were investigated by varing *x* ratio ($x = [Al]/[In + Al]$) from 0 to 0.75. The structural, optical and electrical properties of films were studied, respectively, using X-ray diffraction, Raman spectroscopy, UV-visible spectrophotometer, Hall-effect and four-point probe method. The X-ray diffraction analysis proved that the film deposited at $x = 0.75$ present Cu(In,Al)Se_2 single phase in its chalcopyrite structure and with preferred orientation along [112] direction, however the others films show the main Cu(In,Al)Se_2 chalcopyrite with the formation of In_2Se_3 as a secondary phase.

The band gap energy of the films was controlled from 1.17 to 1.65 eV by adjusting the Al and In concentrations in the precursor solutions. The Raman analysis revealed that all the films mainly consist of a chalcopyrite structure and the film deposited at $x = 0.25$ contain the ternary compounds $CuAlSe_2$ as secondary phase. This last film showed n-type conduction while the rest of the films showed p-type conduction. The electrical resistivity is in the range of 0.06–1.9 Ω cm.

1. Introduction

Cu(In,Al)Se_2 abbreviated as CIASe, is considered as one of the most promising materials and an alternative candidate to wider band gap Cu(In,Ga)Se_2 and $CuIn(S,Se)_2$ absorber thin film solar cells, because it requires relatively smaller alloy concentration than gallium or sulphur to achieve a similar band gap [1], and it can be obtained both as p and n conduction types. Furthermore, it is a much cheaper and an abundant material [1,2]. The optical band gap of $Cu(In_{1-x}Al_x)Se_2$ semiconductor can be controlled from 1 eV (for $x = 0$) to 2.7 eV (for $x = 1$) by the partial substitution of indium by aluminum [3]. The photovoltaic conversion efficiency has already achieved 16.9% using $Cu(In_{1-x}Al_x)Se_2$ material with 13% Al substitution and with a band gap of 1.16 eV [4,5]. These progresses open up new perspectives to enhance the solar cells efficiency.

* Corresponding author at: Faculty of Sciences, Mohammed Boudiaf University, M'Sila 28000, Algeria.
E-mail address: meglali2@yahoo.fr (O. Meglali).

http://dx.doi.org/10.1016/j.ijleo.2017.04.072
0030-4026/

Table 1
Composition of different used baths and the films growth rate prepared by these baths.

Precursor based solution	Bath			
	(a)	(b)	(c)	(d)
$CuCl_2$ (mM)	10	10	10	10
$InCl_3$ (mM)	20	15	10	5
$AlCl_3$ (mM)	0	5	10	15
SeO_2 (mM)	20	20	20	20
x = [Al]/[Al + In]	0	0.25	0.5	0.75
Growth rate (nm/s)	5.5	4.4	3.9	4.9

Cu(In,Al)Se_2 thin films have been prepared by several techniques including evaporation [5–8], chemical bath deposition [2], electrodeposition [1,3], pulsed laser deposition [9], selenization of evaporated precursors [10], magnetron sputtering combined with thermal selenization process[11,12], and so on. When compared to other methods, the electrodeposition one has number of advantages such as easy to carry out, non-vacuum process, required low processing temperature and scalability for large area thin films deposition [13]. However, electrodeposition of quaternary alloys is slightly difficult, because of a great difference in deposition potential of the precursors, and owing to the possibility of the creation of intermediate phases throughout electrodeposition [14].

However, few studies have been devoted to the growth of Cu(In,Al)Se_2 with the electrodeposition technique. D. Pracher et al. [15] and K.H. Huang et al. [3] reported the effect of the deposition potential and chemical bath composition on the properties of Cu(In,Al)Se_2 grown on fluorine doped tin oxide and Mo coated soda lime glass substrates, by one step electrodeposition using a three electrode cell configuration. Saturated Calomel Electrode (SCE) is used as the reference electrode. K.H. Huang et al. have added the sodium dodecyl sulfate (SDS) to the precursor based solution. The reference electrode is external impurity sources and hence could poison the bath, and drastically reduce the efficiency of solar cells fabricated [16,17].

In this research work, we investigated the effect of Al and (In + Al) concentrations in precursor solutions on the properties of Cu(In,Al)Se_2 thin films grown by electrodeposition process using two electrode system and without the addition of complexing agents.

2. Experimental details

Cu(In,Al)Se_2 thin films were deposited using a simple two electrodes cell configuration. The working electrode was the ITO coated glass substrate and the counter electrode was a platinum plate. Before the Cu(In,Al)Se_2 electrodeposition, the substrates were ultrasonically cleaned with acetone, washed with distilled water jet and dried.

The electrolytic solution is composed from $CuCl_2$, $InCl_3$, $AlCl_3$ and SeO_2 dissolved in de-ionized water. Films were deposited with various molar ratios of Al to (Al + In) in the solutions, defined as x(x = [Al]/[Al + In]). The [Al + In] concentration is kept constant for all solutions but the amount of [Al] is increased in detriment of [In]. Four electrolytes baths were prepared with x values equal to (a) 0, (b) 0.25, (c) 0.50 and (d) 0.75 (Table 1). The pH of the solutions was adjusted to 2.6. The deposition was carried out at room temperature without stirring and the applied potential was fixed at −7 V [18]. The post-deposited films were subsequently annealed under vacuum at 300 °C during 30 min. The reduction of copper, indium, aluminum and selenium occurs by the following reaction mechanism:

For copper: $Cu^{+2} + 2e^- \rightarrow Cu_{(s)}$

For indium: $In^{+3} + 3e^- \rightarrow In_{(s)}$

For aluminum: $Al^{+3} + 3e^- \rightarrow Al_{(s)}$

For selenium: $HSeO_2^+ + 4H^+ + 4e^- + OH^- \rightarrow H_2SeO_3 + 4H^+ + 4e^- \rightarrow Se_{(s)} + 3H_20$

The crystalline structure was studied by means of X-ray diffraction using $CuK_{\alpha 1}$ radiation (λ = 1.54056 Å). From the corrected full width at half maximum (FWHM) noted as β of the maximum intensity peak of the X-ray diffraction patterns, one can estimate the average crystallite size C_s of the samples with the Scherrer's formula [19]:

$$C_s = \frac{0.9\lambda}{\beta \cos\theta} \tag{1}$$

where λ is the wavelength of CuK_α radiation, θ is the Bragg angle. The values of θ and β were estimated by fitting a Lorentz function to the maximum intensity peak of X-ray diffraction pattern.

And from the (hkl) planes the lattice constants a and c were evaluated using the standard formulas:

$$d_{hkl} = \frac{n\lambda}{2\sin\theta} \tag{2}$$

$$\frac{1}{d_{hkl}^2} = \frac{h^2 + k^2}{a^2} + \frac{l^2}{c^2} \tag{3}$$

where n is the order of diffraction, d_{hkl} is d-spacing of the (hkl) peak and (h k l) are the Miller indices.

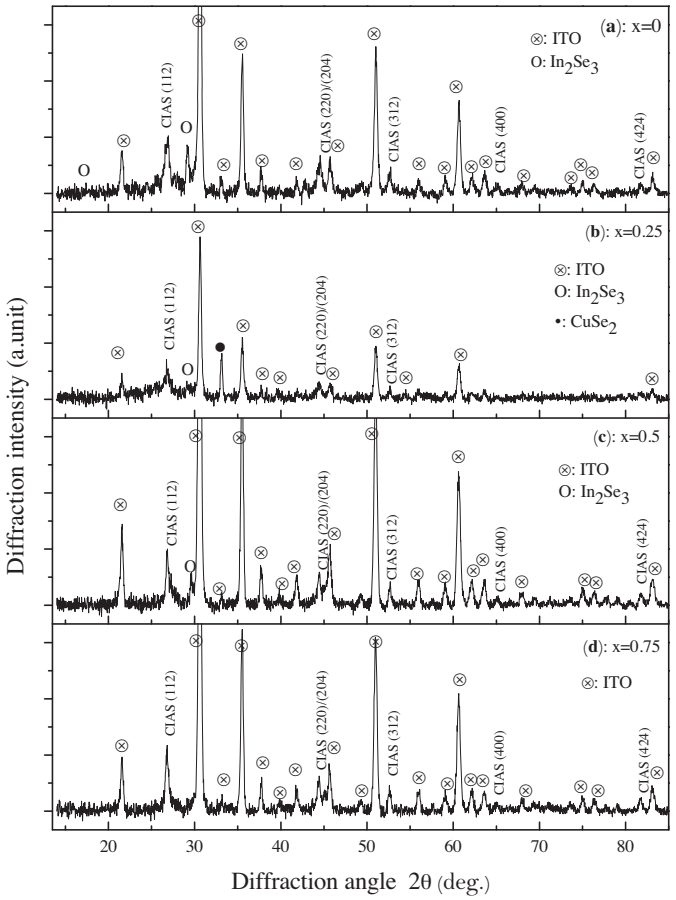

Fig. 1. X-ray diffraction patterns of annealed Cu(In,Al)Se_2 films deposited on ITO coated glass substrate as function of *x* molar ratio in the precursor solution (a) 0, (b) 0.25, (c) 0.50 and (d) 0.75. The diffraction peaks identified from the ITO phase are marked by ⊗ symbol.

On the other hand, using the average crystallite size C_s, the dislocation density δ and the strain ϵ in the films are evaluated respectively using the following formulas [20]:

$$\delta = \frac{1}{C_s^2} \tag{4}$$

$$\varepsilon = \frac{1}{4}\beta \cos\theta \tag{5}$$

The optical transmittance was recorded at room temperature, in the wavelength range from 200–1800 nm by means of ultraviolet-visible-near-infrared (UV-Vis-NIR) spectrophotometer (Shimadzu UV-3101). The films thicknesses were determined by means of profilometer stylus displacement. The values of the growth rate are reported in Table 1. Raman spectra of the films were performed at room temperature using micro Raman system (SENTERRA Raman Microscope) with a 532 nm wavelength as the light excitation source and with a data resolution of 0.5 cm^{-1}. The electrical characterization was carried out at room temperature with Ecopia HMS-3000 Hall Measurement System.

3. Results and discussion

3.1. X-ray diffraction analysis

The X-ray diffraction patterns of films deposited with various molar ratios $x = [Al]/[Al + In]$ in solutions are shown in Fig. 1(a–d) ((a): 0, (b): 0.25, (c): 0.5 and (d): 0.75). Since no JCPDS card is available for the quaternary Cu(In,Al)Se_2, however the JCPDS cards for $CuInSe_2$ (40-1487) [21] and $CuAlSe_2$ (75-0101) [22] are used to identify the phases in the prepared films.

The lines observed respectively in $2\theta \approx 21.26^\circ$, 30.22°, 35.26°, 37.66°, 50.5° and 60.3° (and indexed by ⊗ symbol) are characteristic of the ITO phase (JCPDS # 76-0154) [23]. We found that, after annealing of as deposited films, the ITO substrates keep its initial structure.

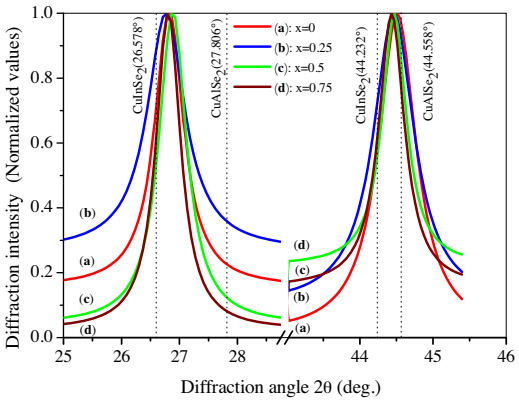

Fig. 2. X-ray diffraction scans reflecting only the sections of the (112) and (220)/(204) position peaks for Cu(In,Al)Se_2 films. The peaks are lorentzian fitted and their intensities are normalized to 1. The vertical dashed lines indicated the position of (112) peak for chalcopyrite $CuInSe_2$ and $CuAlSe_2$ materials.

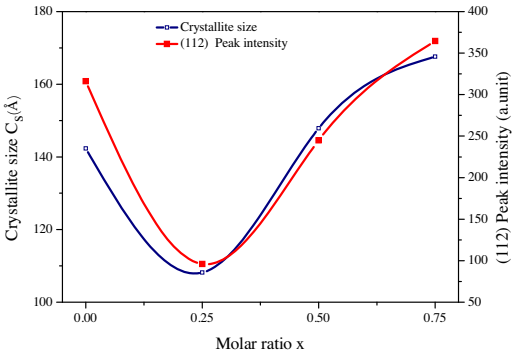

Fig. 3. Variation of crystallite size and (112) peak intensity versus *x* molar ratio in the precursor solution.

After annealing treatment, diffraction spectra revealed that all films are polycrystalline and show the peaks located at $2\theta \approx 26.86^\circ$, 44.37°, 52.59°, 64.76° and 81.62°. These peaks correspond to the most intense peaks of the tetragonal phase of the Cu(In,Al)Se_2 in its chalcopyrite structure (JCPDS # 40-1487) [21]. They correspond to the following lattice planes (112), (220)/(204), (312), (400) and (424).

Fig. 2 shows the X-ray diffraction scans reflecting only the sections of the scan 25°–28.50° and 43°–45.50° for the elaborated films related to different *x* ratio. The expected diffraction angles of the peaks due to $CuInSe_2$ and $CuAlSe_2$ are represented by dashed vertical lines. As can be seen from this figure, the peaks position of these two most intense (112) and (220)/(204) are found to lie between those of $CuInSe_2$ and $CuAlSe_2$. The peaks shifts lead to the change of *d*-spacing and the lattice constants. On the other hand, no additional peak corresponding to Al was observed in the X-ray diffraction patterns, indicating the substitution of Al ions at the In sites in $CuInSe_2$ lattice.

As can be seen in Fig. 1(a–c), in addition to Cu(In,Al)Se_2 and ITO reflection peaks, the films deposited at $x = 0$, 0.25 and 0.50 show additional peaks situated at $2\theta \approx 17.56$ and 29.28°, these lines are assigned to the In_2Se_3 binary phase [24]. Since for these chemical baths, a proportion of the In and Se ions are reacted to form the In_2Se_3 phase.

Furthermore, the film deposited from $x = 0.25$ show a relatively intense peak at 32.94°, this line is attributed to the $CuSe_2$ phase (JCPDS # 26-1115). The appearance of the two secondary phases in this film explains the decrease in the (112) peak intensity of Cu(In, Al)Se_2 (Fig. 3).

No peaks related to any secondary phases are detected in the diffractogram of the film deposited at $x = 0.75$ and the intensity of the (112) peak is higher for this film (Fig. 3), indicating that this film seems to have better crystallinity.

The texturing coefficient R_I is defined as the ratio of (112) peak intensity to the sum of the intensities of all peaks in the X-ray pattern [25]. Calculation results of the rate R_I for $x = 0$, 0.25, 0.5 and 0.75 are respectively 0.52, 0.40, 0.60 and 0.66, so it is found that (for $x \neq 0$) the R_I coefficient increases as the molar ratio increases, and in the other hand, these values are greater than the reference value (0.2), indicating that the [112] axis is not only the most intense peak, but it is also the high degree of preferred orientation of the developed layers. This axis of growth is found to be beneficial for the lattice matching between Cu(In,Al)Se_2 and other II-VI semiconductor.

The variation of the average crystallite size C_s versus *x* ratio is shown with the intensity of the (112) peak in Fig. 3. As can be seen from this figure, the crystallite size and the intensity of the (112) peak have similar behavior. In the first region $0 \leq x \leq 0.25$, the crystallite size decrease with *x* from about 142 to 108 Å, this confirms the deterioration in the crystallinity of

Table 2
The lattice constants (a and c), tetragonal distortion (η), strain (ε) and dislocation density (δ) versus x molar ratio in the precursor solution.

x molar ratio	a (Å)	c (Å)	$\eta = \frac{c}{2a}$	Dislocaltion density δ ($\times 10^{15}$ lines m^{-2})	Strain ε ($\times 10^{-3}$ %)
0	5.755	11.509	0.999	4.9	2.5
0.25	5.761	11.554	1.002	8.5	3.3
0.5	5.761	11.415	0.991	4.5	2.4
0.75	5.764	11.490	0.997	3.5	2.1

the film deposited with $x = 0.25$ due to the formation of secondary phases In_2Se_3 and $CuSe_2$ as observed in X-ray diffraction. However, it is an increasing function of x in the second region; and it achieved its maximum value for $x = 0.75$. The average crystallite size increasing is a manifestation of the decreased density of various defects such as dislocation, vacancies and grains boundaries; this lead to atoms rearrangement in the structure and confirms the high crystallinity of the film elaborated from $x = 0.75$.

The lattice constants a and c, tetragonal distortion η, dislocation density δ and internal strain ε are calculated respectively from Eqs. (2)–(5) and the obtained results are listed in Table 2.

The lattice constants a and c obtained for $x = 0.25$ (i.e. for $CuInSe_2$) agree well with those reported in the literature [26,27]. For other values of x, the lattice constants are also comparable with that reported for Cu(In,Al)Se_2 materials. We found that, the lattice constants of the deposited films does not follow the Vegard's law, this is also due to the presence of secondary phases as proved by X-ray analysis. The obtained values are in good agreement with that reported in the literature, Sugiyama et al. [28] have reported respectively the values of $a = 5.73$ Å and $c = 11.40$ Å for Cu(In,Al)Se_2 thin films prepared by selenization.

The variations of the dislocations density and the internal strain versus the x ratio have similar pace and are inversely proportional to the crystallite size. In the region ($x \leq 0.25$) we note that the dislocations density and strain are increasing function of the x ratio, and they are decreasing in the region $0.25 \leq x \leq 0.75$.

Moreover, the values obtained for the tetragonal distortion ranging between 0.99 and 1.01. The obtained values are in good agreement with that reported in the literature and the lattice tends to an ideal chalcopyrite [29].

3.2. Optical characterization

The quaternary Cu(In, Al)Se_2 is a direct band gap semiconductor [8,30], so the energy band gap E_g can be deduced from x intercept of the linear extrapolation of the curve that shows the variation of $(\alpha h\nu)^2$ versus photon energy ($h\nu$) (Fig. 4(a–d)) using the well-known relationship [3,31]:

$$\alpha = \frac{C}{h\nu}(h\nu - E_g)^{1/2} \tag{6}$$

where α is the absorption coefficient, $h\nu$ is the incident photon energy, E_g is the band gap and C is a constant which depends on the transition nature, effective mass and refractive index.

The obtained values of energy band gap E_g are reported as a function of x ratio in Fig. 5. As shown in this figure, the band gap energy increased nonlinearly with increasing x ratio in the precursor solutions, this confirms the effective incorporation of aluminum in the films and can be correlated with the X-ray analysis results. Its values lie between 1.17 and 1.65 eV, which are in good agreement with the reported ones by many workers on Cu(In,Al)Se_2 films [3,7]. Wei Cheng et al. [32] have found that the energy band gap increases from 1.25 to 1.8 eV when the [Al]/[Al + In] molar ratio in Cu(In,Al)Se_2 films increases from 0.26 to 0.56.

According to the following equation [8,31]:

$$E_g(x) = (1 - x)E_g(A) + xE_g(B) - bx(1 - x) \tag{7}$$

where $E_g(A)$ is the band gap of $CuInSe_2$ ($x = 0$), $E_g(B)$ is the band gap of $CuAlSe_2$ ($x = 1$), b is the optical bowing parameter ($b = 0.62$) which induces a difference with linear averaged behavior, and x is the aluminum concentration in the semiconductor material. The insert in Fig. 5 shows the theoretical relationship between the energy band gap and [Al]/[Al + In] molar ratio in Cu(In,Al)Se_2 semiconductor. The slight difference between the theoretical and experimental values could be principally due to the presence of the In_2Se_3 as a secondary phase in the films. The increasing of the band gap with x ratio confirms that the variation of the aluminum concentration in the produced films was almost in agreement with those in the electrolytic solutions. By using the obtained values of band gap in Eq. (7) we can deduce the Al concentration in the prepared films, these values are equal to 0.23, 0.44 and 0.65 respectively for $x = 0.25$, 0.50 and 0.75.

3.3. Raman analysis

The Raman spectra of the prepared samples excited by 532 nm Ar-ion laser line, recorded at room temperature in the range of 100–300 cm^{-1}, are presented in Fig. 6(a–d). We found that the spectra of samples deposited from $x = 0$, 0.5, and 0.75 (Fig. 6(a, c, and d)) have the most intense peak at 174 cm^{-1}. Note that this peak is shifted to 186 cm^{-1} for the sample deposited at $x = 0.25$ (Fig. 6(b)). This vibration band is attributed to the A_1 mode, which is the strongest peak characteristic of $A^IB^{III}C_2^{VI}$

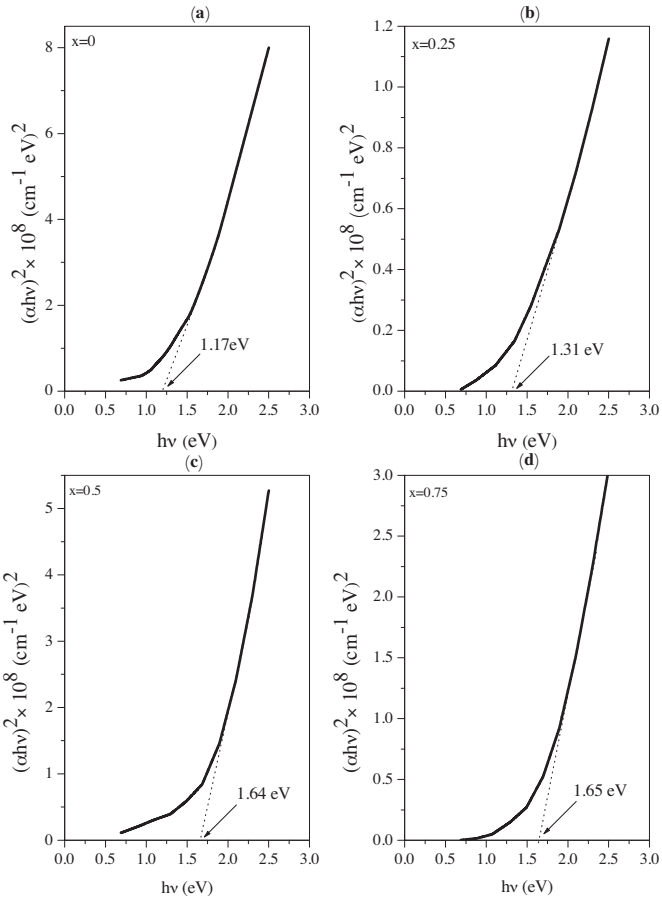

Fig. 4. The square of the measured absorption coefficient $(\alpha h\upsilon)^2$ versus the incident photon energy $(h\upsilon)$ for Cu(In,Al)Se_2 film deposited at different x molar ratio in the precursor solution: (a) 0, (b) 0.25, (c) 0.50 and (d) 0.75.

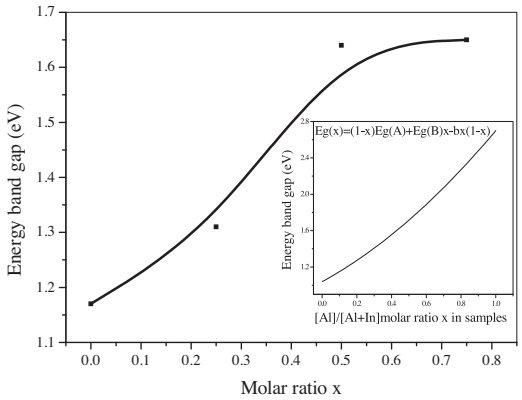

Fig. 5. Variation of the energy band gap E_g with x molar ratio in the precursor solution. The insert shows the theoretical relationship between the energy band gap and [Al]/[Al + In] molar ratio in Cu(In,Al)Se_2 semiconductor.

chalcopyrite compounds [33,34]. The A_1 mode of Cu(In,Al)Se_2 is due to the vibration of Se atoms in the perpendicular direction to the c axis and the Cu, In and Al atoms remain at rest [1].

Olejnicek et al. [4] represented the evolution of the A_1 mode position as function of x = [Al]/([Al] + [In]) ratio and they found that for a ratio ranging from 0 to 1 the position of this peak varies from 172 to 186 cm^{-1}. This indicates that the film deposited at x = 0.25 contain the $CuAlSe_2$ as secondary phase, but this phase was not observed in the X-ray diffraction spectra because it is in small quantities or it is amorphous.

The peak corresponding to A_1 mode of $CuInSe_2$ (x = 0) has a higher intensity as expected.

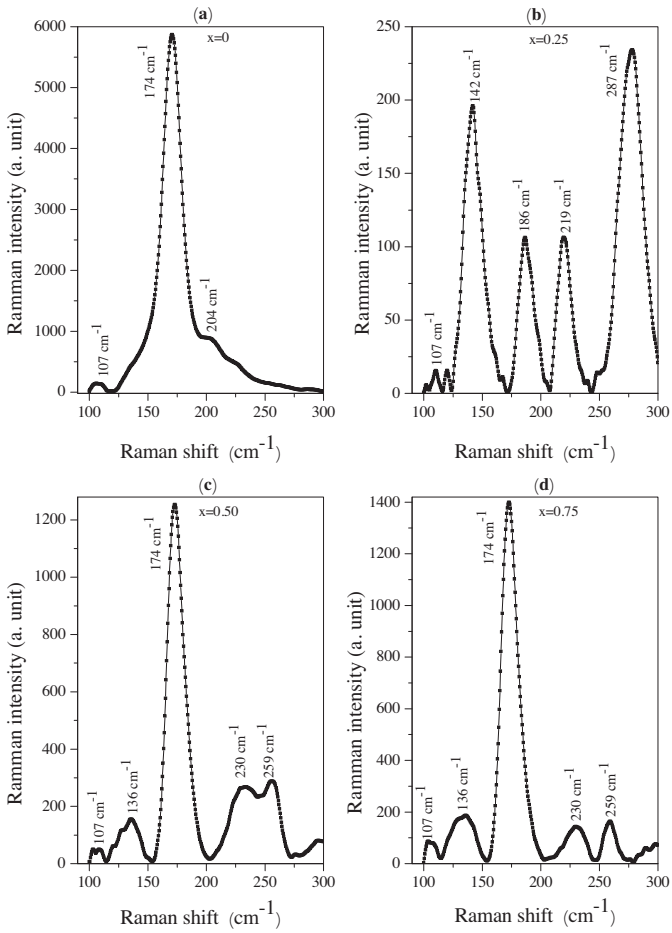

Fig. 6. Raman spectra of Cu(In,Al)Se_2 thin films as function of *x* molar ratio in the precursor solution, (a) 0, (b) 0.25, (c) 0.50 and (d) 0.75.

Table 3
The electrical mobility, the carrier density and the conduction type of Cu(In,Al)Se_2 thin films deposited at different *x* molar ratio in the precursor solution.

Molar ratio *x*	Carrier mobility ($cm^2\ V^{-1}\ s^{-1}$)	Conduction type	Carrier density (cm^{-3})
0	445	p	2.06×10^{17}
0.25	315	n	4.05×10^{10}
0.50	1.94×10^3	p	6.15×10^{15}
0.75	2.06×10^2	p	1.59×10^{16}

The Raman peaks observed at around 219 and 232 cm^{-1} (Fig. 6(b–d)) are assigned to the B_2 vibration mode as reported by [4,35,36]. The peak detected at 260 cm^{-1} is characteristic of Cu–Se binary phase which contains CuSe and $Cu_{2-x}Se$ and its cancelation can be carried out by adequate thermal annealing or by dipping the films in KCN solution [35,37,38].

The peaks appeared at 107, 142 and 204 cm^{-1} match well with the modes detected in the In_2Se_3 phase, this phase is also identified by the X-ray diffraction for the films deposited at $x = 0$, 0.25 and 0.50. These peaks are respectively the vibration modes of A_1 (LO + TO), A_1 (TO) and A_1 (LO) of the In_2Se_3 phase [39,40]. The peak at 107 cm^{-1} is also observed by K.G. Deepa et al. in their work [1] and it is not attributed.

The peaks located at 136 and 287 cm^{-1} are probably due to the presence of complex point defects in the chalcopyrite structure which gives rise to the formation of ordered vacancies compounds (OVCs).

3.4. Electrical characterization

Room-temperature Hall measurements and the four-point probe method are employed for the determination of the conduction type, carrier density, carrier mobility and the electrical resistivity of the prepared Cu(In,Al)Se_2 films. The obtained results are listed as function of *x* ratio in Table 3.

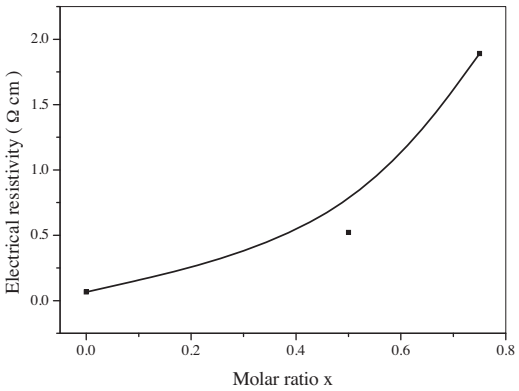

Fig. 7. Variation of the electrical resistivity versus *x* molar ratio in the precursor solution (only for the films having p-type conduction).

It is found that, with the exception of the film deposited at $x = 0.25$ which shows n-type conduction and lower electron density, all the rest samples were p-type conduction. The n-type conduction of the film deposited at $x = 0.25$ is the result of the presence of $CuAlSe_2$ as a secondary phase in this film; this is confirmed by the Raman analysis (the peak centered at 186 cm^{-1} in Fig. 6(b)). A similar observation was reported by Deepa et al. [1], and they explained this by (In + Al) ratio which is higher (≥31.3%) for the films showed n-type conduction.

Fig. 7 has shown the variation of the electrical resistivity of the films having p-type conduction versus the *x* ratio. As can be seen from this figure, the electrical resistivity increases with the *x* ratio, and as expected its behavior is different from that of the crystallite size.

In the first region ($x \leq 0.50$), the crystallite size (Fig. 3), the electron mobility (Table 3) and the electrical resistivity (Fig. 7) increases with the *x* ratio, but the holes concentration decreases, this indicates that the films conductivity in this region is controlled by the carriers concentration.

In the second region ($x \geq 0.50$), we note that, the increase in the electrical resistivity despite the carrier density increasing (see Table 3), we, therefore, find that the electrical conductivity in this region is influenced by mobility rather than by the carrier density.

The obtained values are comparable to those reported in the literature. Reddy et al. [41] and Deepa et al. [1] have reported respectively a value of 140 Ω cm for $CuIn_{0.3}Al_{0.7}Se_2$ thin films prepared by co-evaporation technique and 3 Ω cm for $Cu(In,Al)Se_2$ prepared by one-step electrodeposition.

4. Conclusion

In this paper we studied the effect of Al and In concentration in precursor solutions on the properties of $Cu(In,Al)Se_2$ thin films deposited on ITO substrates by the electrodeposition method. X-ray analysis revealed that the films elaborated with $x = 0.75$ present single phase $Cu(In,Al)Se_2$ in its chalcopyrite structure and with preferred orientation along [112] direction and this film have the better crystalline properties. In the films deposited with $x = 0$, 0.25 and 0.50, In_2Se_3 is present as a secondary phase together with the main $Cu(In,Al)Se_2$ chalcopyrite phase. The chalcopyrite structure of the films was also confirmed through Raman spectroscopy. The band gap energy of the films increased nonlinearly with increasing *x* ratio, it is in the range of 1.17–1.65 eV. The obtained values justify the preferential status of the elaborated thin films as an absorber layer in solar cells applications. Electrical studies show that, with the exception of the film deposited at $x = 0.25$ which show n-type conduction, all the rest samples were p-type conduction.

References

[1] K.G. Deepa, N. Lakshmi Shruthi, M. Anantha Sunil, J. Nagaraju, $Cu(In,Al)Se_2$ thin films by one-step electrodeposition for photovoltaics, Thin Solid Films 551 (2014) 1–7.
[2] B. Kavitha, M. Dhanam, In and Al composition in nano-$Cu(InAl)Se_2$ thin films from XRD and transmittance spectra, Mater. Sci. Eng. B 140 (2007) 59–63.
[3] K.C. Huang, C.L. Liu, P.K. Hung, M.P. Houng, Effect of [Al] and [In] molar ratio in solutions on the growth and microstructure of electrodeposition $Cu(In,Al)Se_2$ films, Appl. Surf. Sci. 273 (2013) 723–729.
[4] J. Olejnicek, C.A. Kamler, S.A. Darveau, C.L. Exstrom, L.E. Slaymaker, A.R. Vandeventer, N.J. Ianno, R.J. Soukup, Formation of $CuIn_{1-x}Al_xSe_2$ thin films studied by Raman scattering, Thin Solid Films 519 (2011) 5329–5334.
[5] S. Marsillac, P.D. Paulson, M.W. Haimbodi, R.W. Birkmire, W.N. Shafarman, High efficiency solar cells based on $Cu(In,Al)Se_2$ thin films, Appl. Phys. Lett. 81 (2002) 1350–1352.
[6] S. Yamada, K. Tanaka, T. Minemoto, H. Takakura, Effect of Al addition on the characteristics of $Cu(In,Al)Se_2$ solar cells, J. Cryst. Growth 311 (2009) 731–734.
[7] Dhananjay, J. Nagaraju, S.B. Krupanidhi, Structural and optical properties of $CuIn_{1-x}Al_xSe_2$ thin films prepared by four-source elemental evaporation, Solid State Commun. 127 (2003) 243–246.

[8] E. Halgand, J.C. Bernède, S. Marsillac, J. Kessler, Physico-chemical characterization of Cu(In,Al)Se_2 thin film for solar cells obtained by selenization process, Thin Solid Films 480–481 (2005) 443–446.
[9] K.H. Kim, Fianti, Growth of single-phase $CuInAlSe_2$ thin films by using pulsed laser deposition and selenization, J. Korean Phys. Soc. 60 (2012) 2001–2006.
[10] S. Martin, C. Guillen, Characterization of chalcopyrite Cu(In,Al)Se_2 thin films grown by selenization of evaporated precursors, Energy Proc. 10 (2011) 182–186.
[11] X. Meng, H. Cao, Deng.F H, W. Zhou, J. Zhang, L. Huang, L. Sun, P. Yang, J. Chu, Structural, optical and electrical properties of $Cu_2FeSnSe_4$ and Cu (In Al)Se_2 thin films, Mater. Sci. Semicond. Process. 39 (2015) 243–250.
[12] M. Jianping, L. Yaming, L. Yanto, Preparation and characterization of the Cu(In,Al)Se_2 absorber, Adv. Electr. Eng. Electr. Mach. 134 (2011) 329–335.
[13] J. Sun, S.K. Batabyal, P.D. Tran, L.H. Wong, Electrodeposition of single phase $CuInSe_2$ for solar energy harvesting: role of different acidic additives, J. Alloys Compd. 591 (2014) 127–131.
[14] A. Chihi, M.F. Boujmil, B. Bessais, Optical and electrical characterization of CIGS thin films grown by electrodeposition route, Optik 127 (2016) 4118–4122.
[15] D. Prasher, P. Rajaram, Growth and characterization of electrodeposited Cu(In,Al)Se_2 thin films, Thin Solid Films 519 (2011) 6252–6257.
[16] I.M. Dharmadasa, R.P. Burton, M. Simmonds, Electrodeposition of $CuInSe_2$ layers using a two-electrode system for applications in multi-layer graded bandgap solar cells, Sol. Energy Mater. Sol. Cells 90 (2006) 2191–2200.
[17] A. Bouraiou, M.S. Aida, E. Tomasella, N. Attaf, ITO substrate resistivity effect on the properties of $CuInSe_2$ deposited using two-electrode system, J. Mater. Sci. 44 (2009) 1241–1244.
[18] A. Bouraiou, M.S. Aida, O. Meglali, N. Attaf, Potential effect on the properties of $CuInSe_2$ thin films deposited using two-electrode system, Curr. Appl. Phys. 11 (2011) 1173–1178.
[19] L.I. Malssel, R. Glang, Handbook of Thin Film Technology, McGraw Hill Book Company, New York, 1970.
[20] M. Dhanam, P.K. Manoj, R.R. Prabhu, High-temperature conductivity in chemical bath deposited copper selenide thin films, J. Cryst. Growth 280 (2005) 425–435.
[21] International Center for Diffraction Data, ICDD, PDF2 Database, file number 40-1487 for $CuInSe_2$.
[22] International Center for Diffraction Data, ICDD, PDF2 Database, file number 75-0101 for $CuAlSe_2$.
[23] International Center for Diffraction Data, ICDD, PDF2 Database, file number 76-0152 for In_2O_3.
[24] O. Meglali, N. Attaf, A. Bouraiou, M.S. Aida, S. Lakehal, One-step electrodeposition process of $CuInSe_2$: deposition time effect, Bull. Mater. Sci. 37 (2014) 1535–1542.
[25] J. Muller, J. Nowoczin, H. Schmitt, Composition, structure and optical properties of sputtered thin films of $CuInSe_2$, Thin Solid Films 496 (2006) 364–370.
[26] E. Yassitepe, W.N. Shafarman, S. Ismat Shah, Microstructure and phase evolution in single phase $CuInSe_2$ particles synthesized using elemental precursors, J. Solid State Chem. 213 (2014) 198–203.
[27] A.A.I. Al-Bassam, Electrodeposition of $CuInSe_2$ thin films and their characteristics, Physica B 266 (1999) 192–197.
[28] M. Sugiyama, A. Umezawa, T. Yasuniwa, A. Miyama, H. Nakanishi, S.F. Chichibu, Growth of single-phase Cu(In,Al)Se_2 photoabsorbing films by selenization using diethylselenide, Thin Solid Films 517 (2009) 2175–2177.
[29] U. Parihar, K. Sreenivas, J.R. Ray, C.J. Panchal, N. Padha, B. Rehani, Influence of substrate temperature on structural, optical, and electrical properties of flash evaporated $CuIn_{0.81}Al_{0.19}Se_2$ thin films, Mater. Chem. Phys. 139 (2013) 270–275.
[30] J. Lopez-Garcia, C. Maffiotte, C. Guillen, Wide-bandgap $CuIn_{1-x}Al_xSe_2$ thin films deposited on transparent conducting oxides, Sol. Energy Mater. Sol. Cells 94 (2010) 1263–1269.
[31] J. López-García, C. Guillén, $CuIn_{1-x}Al_xSe_2$ thin films obtained by selenization of evaporated metallic precursor layers, Thin Solid Films 517 (2009) 2240–2243.
[32] K.-W. Cheng, K. Hinaro, M.P. Antony, Photoelectrochemical water splitting using Cu(In,Al)Se_2 photoelectrodes developed via selenization of sputtered Cu-In-Al metal precursors, Sol. Energy Mater. Sol. Cells 151 (2016) 120–130.
[33] J. Zhang, S. Zhang, H. Zhang, Y. Zhang, Z. Zheng, Y. Xiang, Activated selenium for promoted formation of metal selenide nanocrystals in solvothermal synthesis, Mater. Lett. 122 (2014) 306–308.
[34] A. Eifler, E.A. Kudritskaya, I.V. Bodnar, V. Riede, Infrared and Raman study of lattice vibrations of $CuAlSe_2$ single crystals, J. Phys. Chem. Solids 64 (2003) 1983–1987.
[35] O. Ramdani, J.F. Guillemoles, D. Lincot, P.P. Grand, E. Chassaing, O. Kerrec, E. Rzepka, One-step electrodeposited $CuInSe_2$ thin films studied by Raman spectroscopy, Thin Solid Films 515 (2007) 5909–5912.
[36] X. Li, W. Liu, G. Jiang, D. Wang, C. Zhu, Study of In-Se binaries of In-rich $CuInSe_2$ thin film prepared by selenization after cosputtering, Mater. Lett. 70 (2012) 116–118.
[37] Y.H. Su, T.W. Chang, W.H. Lee, B.H. Tseng, Characterization of $CuInSe_2$ thin films grown by photo-assisted electrodeposition, Thin Solid Films 535 (2013) 343–347.
[38] Z. Zhang, J. Li, M. Wang, M. Wei, G. Jiang, C. Zhu, Influence of annealing conditions on the structure and compositions of electrodeposited $CuInSe_2$ films, Solid State Commun. 150 (2010) 2346–2349.
[39] C. Hwa Ho, M. Han Lin, C. Chi Pan, Optical-memory switching and oxygen detection based on the CVT grown γ- and α-phase In_2Se_3, Sens. Actuators B 209 (2015) 811–819.
[40] R. Lewandowska, R. Bacewicz, J. Filipowicz, W. Paszkowicz, Raman scattering in α-In_2Se_3 crystals, Mater. Res. Bull. 36 (2001) 2577–2583.
[41] Y.B. Kumar Reddy, V.S. Raja, Preparation and characterization of $CuIn_{0.3}Al_{0.7}Se_2$ thin films for tandem solar cells, Sol. Energy Mater. Sol. Cells 90 (2006) 1656–1665.